

Electron-Nuclear Double Resonance of the Self-Trapped Hole in CaF_2 and BaF_2 †‡

ROBERT F. MARZKE

Department of Physics, University of North Carolina, Chapel Hill, North Carolina

AND

ROBERT LEE MIEHER*

Department of Physics, Purdue University, Lafayette, Indiana 47907

(Received 13 January 1969)

The results of an electron-nuclear double-resonance (ENDOR) study of the V_K center (self-trapped hole) in CaF_2 and BaF_2 are reported. In addition to reporting the ENDOR hyperfine constants, some interesting features of ENDOR spectra due to the glide-reflection symmetry of the fluorite lattice are discussed. Also, the large Ba^{++} ion produces effects on the fluorine hyperfine constants that are not observed in the ENDOR spectra of the V_K center in CaF_2 , LiF , or NaF .

I. INTRODUCTION

THIS paper extends the study of V_K centers by electron-nuclear double resonance (ENDOR) previously done in NaCl-type structures¹⁻³ to the fluorite-structured crystals CaF_2 and BaF_2 . The V_K center in these crystals is an F_2^- molecule ion sharing two halogen ion sites in a (001) direction. It has an unpaired spin in a σ_u orbit, which has a large hyperfine interaction with the two spin- $\frac{1}{2}$ fluorine nuclei of the molecule, resulting in a strongly anisotropic four-line electron-spin-resonance (ESR) spectrum, as shown, for example, in Fig. 1. Hayes and Twidell⁴ first observed the V_K spectrum in CaF_2 ; the spectrum for BaF_2 is very similar.⁵

II. EXPERIMENT

The samples were cut from optical quality CaF_2 and BaF_2 rods grown by Optovac, Inc., with 0.05% doping of Tm^{3+} , which had their long axis in either a [100] or a [110] direction. Accurate orientation was achieved using the strongly angular-dependent approach of the R_1 and R_2 ESR lines near 90° (see Fig. 1).

X irradiation at liquid-nitrogen temperature at 70 kV, 30 mA (Muller MC150) for about 1 h nearly saturated V_K center production in CaF_2 , but several hours of irradiation were needed for BaF_2 . The ESR and ENDOR spectra were taken on an X-band superheterodyne spectrometer described in earlier papers,¹⁻³ this spectrometer compensates for drifts during the sweep of an ENDOR spectrum by locking to the resonant frequency of the signal cavity. ENDOR measure-

ments were made on the R_1 and R_3 lines, the former's strong angular dependence making easy the selection of the desired one of three V_K center orientations. The R_3 line occurring near $g=2$ was usually difficult to separate from the many other lines in this region except at small angles, but for CaF_2 selective bleaching of unwanted centers by polarized light near $350 \text{ m}\mu$ helped to clarify the ESR spectrum. This did not work in BaF_2 and eventually for both substances we used the previously determined g tensor to predict the R_3 -line position (in proton probe frequency units) at each angle.

III. RESULTS AND DISCUSSION

Figure 2 shows the nuclei surrounding the V_K center in the fluorite-structure crystals. The unpaired electron spin has hyperfine interactions with the two molecular nuclei and the lattice nuclei. The spin Hamiltonian is^{1,2}

$$H = \beta_0 \mathbf{S} \cdot \mathbf{g} \cdot \mathbf{H}_0 + h \mathbf{S} \cdot [\mathbf{T}_1 \cdot \mathbf{K}_1 + \mathbf{T}_2 \cdot \mathbf{K}_2] - h \gamma_F (\mathbf{K}_1 + \mathbf{K}_2) \cdot \mathbf{H}_0 + h \sum_n \mathbf{S} \cdot \mathbf{A}_n \cdot \mathbf{I}_n - h \gamma_n \mathbf{I}_n \cdot \mathbf{H}_0,$$

where \mathbf{S} is the electron spin, \mathbf{T}_1 and \mathbf{T}_2 are the molecular fluorine hyperfine tensors, \mathbf{A}_n are the hyperfine constants of the lattice nuclei, \mathbf{K}_1 and \mathbf{K}_2 are the molecular fluorine spins, \mathbf{I}_n are the lattice nuclear spins, and the

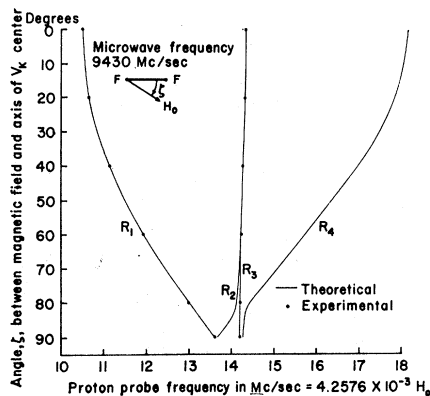


FIG. 1. Angular dependence of the ESR spectrum of the V_K center in CaF_2 ; Hayes and Twidell (Ref. 4).

† Work supported by the National Science Foundation under Grant Nos. NSF-GP-53 and NSF-GP-3385 at Columbia and NSF-GP-4860 at Purdue.

‡ Based upon a thesis submitted by R. F. Marzke in partial fulfillment of the requirements for the Ph.D. degree at Columbia University.

* Alfred P. Sloan Foundation Fellow.

¹ (a) R. Gazzinelli and R. Mieher, Phys. Rev. Letters **12**, 644 (1964); (b) Phys. Rev. **175**, 395 (1968).

² (a) I. Bass and R. Mieher, Phys. Rev. Letters **15**, 25 (1965); (b) Phys. Rev. **175**, 412 (1968).

³ (a) D. F. Daly, Ph.D. thesis, Columbia University, 1966 (unpublished); (b) D. F. Daly and R. Mieher, Phys. Rev. **175**, 395 (1968).

⁴ W. Hayes and J. W. Twidell, Proc. Phys. Soc. (London) **79**, 1295 (1962).

⁵ Y. Kazumata, Phys. Status Solidi **26**, K119 (1968).

TABLE I. Experimental results for hyperfine tensors of nuclei.

Nuclear site	Hyperfine constant ^a (Mc/sec)						Euler angles ^b (deg)			Contact interaction ^a (Mc/sec)
	A_x	A_y	A_z	Anisotropic part			ψ	θ	δ	
				B_x	B_y	B_z				
A (CaF ₂)	0.54	0.54	43.36	-14.27	-14.27	28.55	90.0	-45.0	-90.0	+14.81
A (BaF ₂)	-1.5	-0.5	5.32	-2.6	-1.6	4.21	90.0	-45.0	-90.0	+1.11
	±0.1	±0.1		±0.1	±0.1					±0.08
B (CaF ₂)	4.04	-2.72	-4.64	5.15	-1.61	-3.53	88.0	87.0	-3.0	-1.11
							±1.0	±1.0	±1.0	
B (BaF ₂)	3.30	-1.60	-2.06	3.42	-1.48	-1.94	73.5	86.0	-1.5	-0.12
							±1.0	1.0	±1.0	
C (CaF ₂)	-1.1	1.84	-0.82	-1.1	1.87	-0.8	90.0	-45.0	-104.0	-0.0
	±0.2		±0.02	±0.2		±0.2			±2.0	±0.1
C (CaF ₂)	-1.0	1.56	-1.1	-0.8	1.75	-0.9	90.0	-45.0	-101.0	-0.2
	±0.2		±0.2	±0.2		±0.2			±2.0	±0.1
C (BaF ₂)	-1.00	0.5	-1.34	-0.39	1.1	-0.73	90.0	-45.0	-96.5	-0.6
	±0.08	±0.1	±0.08	±0.08	±0.1	±0.08			±2.0	±0.1
C (BaF ₂)	0.0	2.64	-0.44	-0.7	1.91	-1.17	90.0	-45.0	-130.0	+0.7
	±0.3	±0.08	±0.08	±0.3	±0.08	±0.08			±1.0	±0.2

^a All experimental hyperfine constants are assigned an error of ± 0.04 Mc/sec unless otherwise specified.

^b Euler angles are given with respect to the crystalline coordinate system X_c, Y_c, Z_c of Fig. 2 and describe the orientation of the principal axes of only one nucleus.

hyperfine constants (**A** and **T**) and gyromagnetic ratios are in frequency units.

The ENDOR hyperfine interaction is also frequently written

$$\mathbf{I} \cdot \mathbf{A} \cdot \mathbf{S} = a \mathbf{I} \cdot \mathbf{S} + \mathbf{I} \cdot \mathbf{B} \cdot \mathbf{S},$$

where a is the isotropic Fermi constant interaction and **B** is the anisotropic part of the hyperfine tensor. The experimental ENDOR hyperfine constants are listed in Table I. The ESR constants are given in Refs. 4 and 5.

The ENDOR frequency for a given nucleus is (in zero order¹)

$$\nu_n = |\gamma_n H_0 - m_s W|,$$

where $m = \pm \frac{1}{2}$, $W = A_x h_x^2 + A_y h_y^2 + A_z h_z^2$, and h_i is the direction cosine between H_0 and A_i principal axis. Because of the approximate symmetry about $\gamma_n H_0$ of the ENDOR lines for the two m_s states (see Fig. 3),

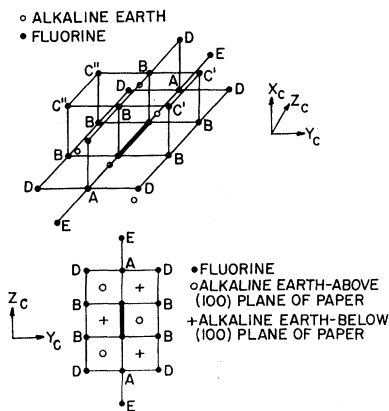


FIG. 2. Nuclei surrounding the V_K center in fluorite-structure crystals. (Crystal axes are labeled X_c, Y_c, Z_c .)

and since the magnetic field H_0 is a function of angle for the ESR spectra (Fig. 1), the ENDOR data in the figures are plotted as $\nu_n - \gamma H_0$.

Fitting the spectrum of each nucleus to a spin Hamiltonian was done by computer programs developed earlier by Bass² and by Dakss.⁶ The latter's program was essential for fitting nuclei having no principal planes determined by symmetry, since it allowed arbitrary orientation, specified by three Euler angles, of the principal axes (x, y, z) of the hyperfine tensor A with respect to the crystal axes (X_c, Y_c, Z_c) as shown in Fig. 4.

The easiest lines to interpret are due to the lattice nuclei nearest the V_K center. These nuclei produce ENDOR lines away from the "central packet" for most orientations. The central packet is the almost

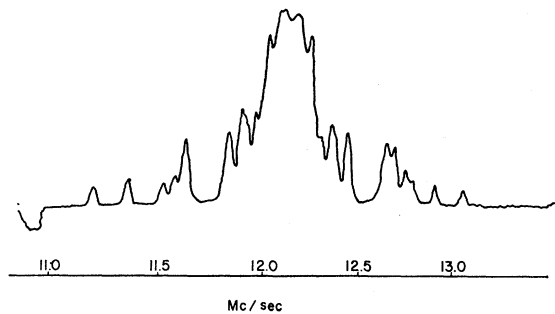


FIG. 3. Example of typical ENDOR data. The field angle is 84° from the V_K axis in the (110) rotation in CaF₂. The frequency is in Mc/sec.

⁶ (a) M. L. Dakss, Ph.D. thesis, Columbia University, 1966 (unpublished); (b) M. L. Dakss and R. Mieher, Phys. Rev. Letters **18**, 1056 (1967).

continuous spectrum of overlapping lines at about 12 Mc/sec in Fig. 3 and is due to many distant nuclei.

Assigning a set of observed ENDOR lines to a set of lattice nuclei surrounding the center is possible for V_K centers because of the strong anisotropy of A for most nuclei and because of the rapid decrease of the wave function with distance away from the molecule. Symmetry arguments, involving lattice equivalence in a magnetic field, generally provide the identification unambiguously. Because of the difference between the NaCl and the fluorite structures, and because of some new effects in the V_K center ENDOR spectra, a description of the identification process is given here.

The problem is complicated by the fluorite lattice possessing two magnetically nonequivalent types of centers in a $\langle 001 \rangle$ direction, which are exchanged by a glide reflection in a $\{100\}$ plane. This produces a doubling of some ENDOR lines for some field rotations. Also, two important sets of nuclei labeled B and D have no principal axes determined by symmetry. The A , C , and E nuclei have $\{110\}$ principal planes which were obvious field rotation planes. The B and D nuclei would have $\{100\}$ principal planes if the alkaline-earth ions were absent from the simple cubic fluorine lattice, so the $\{100\}$ field rotations were also taken.

The fluorine nuclei labeled A in Fig. 2 are inversion-equivalent and should give only one ENDOR line for each m_s state for all field angles. The angular dependence of these lines in CaF_2 was expected to resemble closely that of the lines from a similar pair of nuclei on the axis of the V_K center in LiF. The observed ENDOR lines in the (110) rotation⁷ of Figs. 5(a) and 5(b) indeed resemble the lines of this type of nucleus in LiF, given in Fig. 17 of Ref. 1(b). The angular dependence of the ENDOR spectra for the A nuclei does not show the usual symmetry about γH because of the very large hyperfine interaction (43

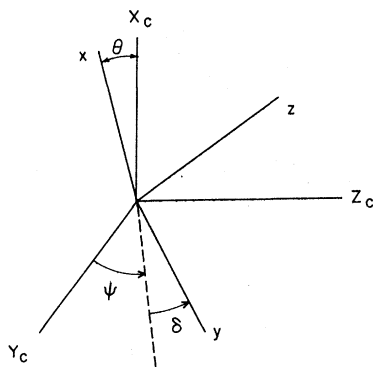


FIG. 4. Euler angles chosen by Dakss (Ref. 6) describing the orientation of the nuclear-hyperfine-tensor principal axes (x, y, z) with respect to the crystal axes (X_c, Y_c, Z_c).

⁷ All references to planes and directions for the rest of the paper assume the F_2^- axis to be in the $[001]$ direction.

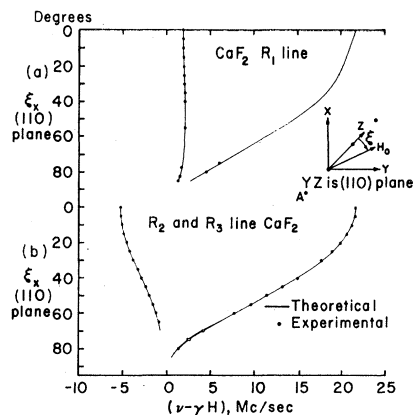


FIG. 5. (a) Angular dependence of the R_1 ENDOR lines of the A nuclei in CaF_2 for the (110) rotation. (b) Angular dependence of the R_2 and R_3 ENDOR lines of the A nuclei in CaF_2 for the (110) rotation. [The (X, Y, Z) axes are not the same as (X_c, Y_c, Z_c) , but are rotated by 45° about the Z_c so that YZ is a (110) plane.]

Mc/sec) for the field parallel to the V_K axis. This large hyperfine interaction even splits the V_K ESR in CaF_2 , as noted by Hayes and Twidell.⁴ The small perpendicular hyperfine constants (0.54 Mc/sec) for the A nuclei were observed to be equal to within the ENDOR linewidth of about 40 kc, even though axial symmetry is not required by the twofold rotational symmetry of the defect.

When the field makes an angle of about 75° with the V_K axis, the high-frequency ENDOR line taken on the R_3 ESR line for the (110) rotation⁷ splits into two lines (see Fig. 5). The A ENDOR line of the R_1 line does not, however. At about this angle the R_2 and R_3 lines in the ESR spectrum also begin to overlap, each being several gauss wide. It appears that the two overlapping ESR lines give slightly different ENDOR frequencies for the A nuclei. Diagonalization of the ENDOR Hamiltonian matrix, with the Hayes Twidell⁴ ESR spin-Hamiltonian parameters plus hyperfine constants adjusted to give the best fit to the A lines, does indeed predict the observed line doubling near 75° .

The eight B nuclei are all hyperfine-equivalent in the lattice because of $(\bar{1}\bar{1}0)$ and (110) reflection planes⁷ through the V_K axis (see Fig. 2). Pairwise inversion equivalence should produce four lines (for each m_s state) for a general magnetic field direction, two lines for the field in either reflection plane, and only one line for the field along the V_K axis. Figure 6(a) shows the angular dependence of the ENDOR spectra for the B nuclei for a rotation of magnetic field from $[001]$ to $[010]$. There are four lines for this rotation, which combine to two lines for the field perpendicular to the V_K axis and to one line for the field along the V_K axis.

There is a (001) reflection plane of the lattice and V_K center perpendicularly bisecting the molecular axis at the inversion center. For a rotation from

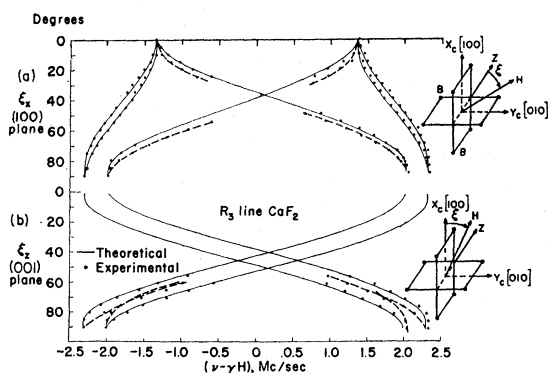


FIG. 6. (a) Angular dependence of the R_3 ENDOR lines of the B nuclei in CaF_2 for the (100) rotation. (Dashed lines show trend of those experimental points for which a theoretical comparison curve was not calculated.) (b) Angular dependence of the R_3 ENDOR lines of the B nuclei in CaF_2 for the (001) rotation.

[100] to [010] in the (001) reflection plane the (110) reflection plane makes the angular dependence symmetrical about 45° [Fig. 6(b)]. For this rotation only two lines (for each m_s state) are expected if we consider only a single V_K center. However, in Fig. 6(b) we have four lines instead of the expected two. The explanation lies in the existence of two types of magnetically distinct V_K centers in the lattice. The two types of centers have the same axis direction and are related by glide-reflection symmetry. The two types of centers are reflection-equivalent for the field in the (100) rotation plane of Fig. 6(a) but are not for the (001) rotation of Fig. 6(b) and the line doubling results.

There are two sources of ambiguity in assigning hyperfine constants to the B 's. The first arises from the symmetry of the lattice and makes it impossible to distinguish experimentally between two assignments of hyperfine constants for the two axes which, for the four B 's in the (100) plane, lie near that plane (and would lie in it if the Ca or Ba ions were not present).

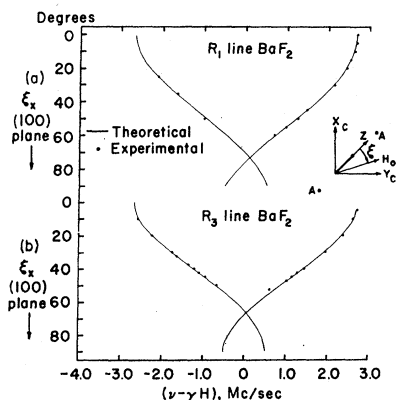


FIG. 7. (a) Angular dependence of the R_1 ENDOR lines of the A nuclei in BaF_2 for the (100) rotation. (b) Angular dependence of the R_3 ENDOR lines of the A nuclei in BaF_2 for the (100) rotation.

Because of the (001) reflection plane of the V_K center, there are two arrangements of the two axes that would produce the same ENDOR spectrum.

The second ambiguity arises because the principal axes of the B nuclei in CaF_2 all lie only a few degrees away from the [100], [010], and [001] crystal axes, i.e., all Euler angles are near 0° or 90° . If the positive ions of the lattice have only a small effect on the hyperfine tensor, one axis for the four B 's in the (100) plane would be expected to be close to the [100] crystal axis. The other two principal axes, lying nearly in the (100) plane, have no fixed orientation by symmetry. Thus it is not clear which lines belong to the slightly tilted first principal axis and which to the other two near the (100) plane, because the Euler angles involved are all so small (see Fig. 3). It is possible to fit the data to a spin Hamiltonian in two ways, within the experimental error, by interchanging the assignments of the hyperfine constants.

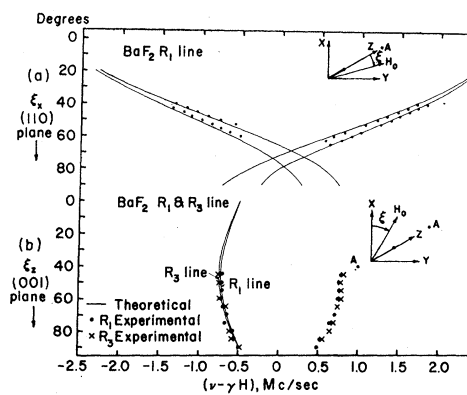


FIG. 8. (a) Angular dependence of the R_1 ENDOR lines of the A nuclei in BaF_2 for the (110) rotation. (b) Angular dependence of the R_3 ENDOR lines of the A nuclei in BaF_2 for the (001) rotation.

The R_1 - and R_3 -line ENDOR spectra for the A nuclei of the V_K center in BaF_2 for the (100) and (110) rotations are given in Figs. 7, 8(a), and 8(b). The parallel hyperfine constant is much smaller in BaF_2 than in CaF_2 (5.32 instead of 43.36 Mc/sec) and it produces no observable hyperfine splitting in the ESR spectrum. The lines in the (100) rotation (Fig. 7) from parallel to perpendicular to the V_K axis are single as expected and disappear into the central packet for the field at angles of about 55° to the V_K axis. Even to fit the large-angle data roughly, we must assume perpendicular hyperfine constants of the opposite sign to the parallel one and of magnitude approximately 1.0 Mc/sec, so that for the field at small angles to the V_K axis the A lines have passed through the central packet and emerged on the opposite side as shown in Fig. 7. However, for the (110) rotation of Fig. 8(a) there are two A ENDOR lines for each m_s state. This line doubling is again due to the two types of V_K centers

related by glide-reflection symmetry as discussed above for the B nuclei. Line doubling should also have occurred for the A nuclei in CaF_2 for the (110) rotation (Fig. 5), but was not observed because the two perpendicular hyperfine constants were equal and small (0.54 Mc/sec). In BaF_2 , however, the perpendicular constants are unequal (-1.5 and -0.5 Mc/sec). The data for the (001) rotation plane in Fig. 8(b) also show that the perpendicular hyperfine constants are unequal. One of the constants (-1.5 Mc/sec) is obtained directly from Fig. 8(b) but the other constant is given by lines under the central packet of the (001) rotation and must be obtained by extrapolation of the data shown in Fig. 8(a). The line doubling does not occur for the (100) rotation (Fig. 7) because of the magnetic reflection equivalence of the two types of V_K centers for this rotation.

The nonaxial nature of the hyperfine tensor for these A nuclei in BaF_2 is interesting because the A nuclei in CaF_2 and all of the other cases¹⁻³ of ENDOR nuclei on

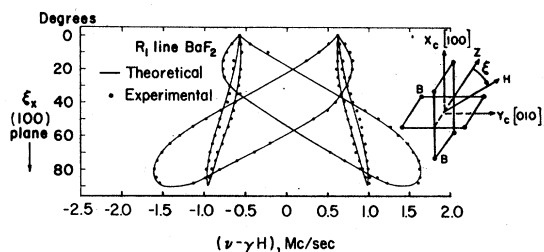


FIG. 9. Angular dependence of the R_1 ENDOR lines of the B nuclei in BaF_2 for the (100) rotation.

the molecular axis have axially symmetrical hyperfine tensors to within 2%. The large Ba^{++} ion evidently produces a large transferred hyperfine interaction for the A fluorines.

The B lines in BaF_2 were not difficult to fit with an ENDOR Hamiltonian, and the principal axes were farther from [100] directions than for CaF_2 . The observed ENDOR spectra are given in Figs. 9 and 10. Although they appear somewhat different because of different values of hyperfine constants, comparison of Figs. 6 and 10 shows that the same symmetry characteristics are present.

We now come to the sets of nuclei more distant from the V_K center, whose spectra present considerable problems in CaF_2 but are surprisingly clear for BaF_2 . We will begin by discussing qualitatively the expected features of the ENDOR spectra of the C nuclei.

The eight C nuclei lie in the $\{110\}$ reflection planes of the defect and are divided into two nonequivalent sets of four by the presence of the alkaline-earth ions. In Fig. 11 the four nuclei in the (110) plane are labeled C' and those in the $(\bar{1}\bar{1}0)$ plane are labeled C'' . Also shown in Fig. 11 are the two different arrangements of

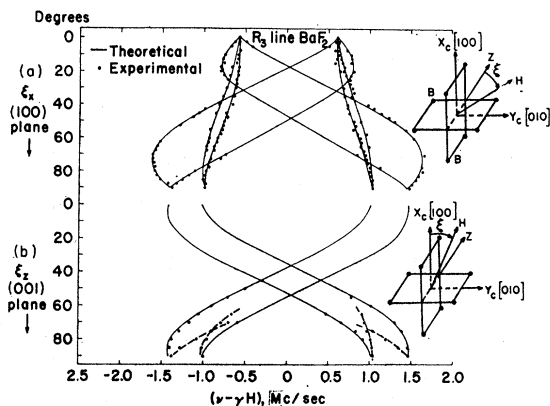


FIG. 10. (a) Angular dependence of the R_3 ENDOR lines of the B nuclei in BaF_2 for the (100) rotation. (b) Angular dependence of the R_3 ENDOR lines of the B nuclei in BaF_2 for the (001) rotation. (Dotted lines show trend of those experimental points for which a theoretical comparison curve was not calculated.)

nearest calcium or barium ions to the V_K center with respect to the C' in the (110) plane and with respect to the C'' in the $(\bar{1}\bar{1}0)$ plane. Again we have two types of V_K centers, so that half have their C' and C'' positions interchanged to $(\bar{1}\bar{1}0)$ and (110). Thus in a particular (110)-lattice plane, half the centers have four equivalent nuclei of the C' type and the other half have four of the C'' type.

Study of the (110)- and $(\bar{1}\bar{1}0)$ -lattice planes shows that a single field rotation from parallel to perpendicular to the V_K axis in a (110) plane gives all the hyperfine constants for both C' and C'' nuclei. This necessarily means a large number of lines for this rotation, and a typical expected spectrum for an arbitrary choice of hyperfine constant values is given in Fig. 12. For example, consider a (110) plane with two V_K centers related by the glide-reflection symmetry having a

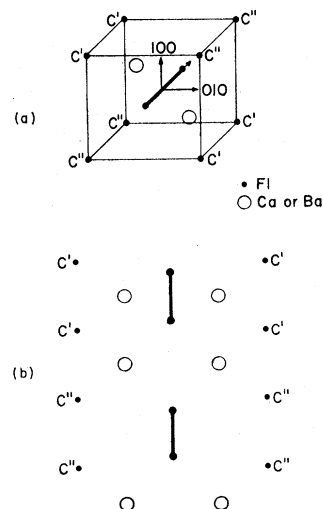


FIG. 11. (a) C' and C'' nuclei around the V_K center. (b) Ions in (110) plane and V_K centers related by glide reflection in (100) plane.

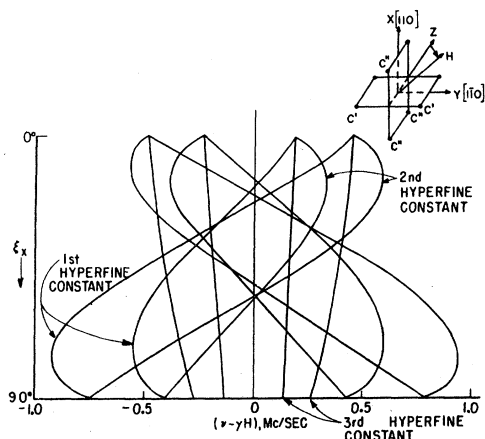


FIG. 12. Typical expected angular dependence of C ENDOR lines for the (110) rotation. Positions where the field is parallel to a principal axis are shown. The lattice diagram shows only one of the two types of centers.

common $[001]$ axis. The plane contains a C' set from one center and a C'' set from the other, and a single field rotation through 90° gives by a (001) -plane reflection both principal hyperfine constants in the (110) plane for both sets. The $(\bar{1}\bar{1}0)$ plane perpendicular to the (110) and passing through the axis also contains both a C'' and a C' set, the C'' being for the V_K center which had C' in (110) and vice versa. When the field is perpendicular to the common (001) axis of the centers, it is along the third principal direction, given by the reflection symmetry, of both the C'' and C' sets in the $(\bar{1}\bar{1}0)$ plane. With the field perpendicular to the V_K axis, the (110) C' lines are equivalent, as are those of the C'' , because of the (001) -lattice reflection plane, containing the field. For all angles of field in the (110) plane, the $(\bar{1}\bar{1}0)$ C'' and C' sets both give one line, because (110) is a lattice-reflection plane. As the field draws nearly parallel to the common axis of the two centers, all the lines from both C'' sets meet, as do those from the C' sets.

Because of the complexity of the spectrum the small hyperfine constants for the C nuclei in CaF_2 made identification difficult. For BaF_2 , however, the hyperfine constants were nearly as large as those of the B

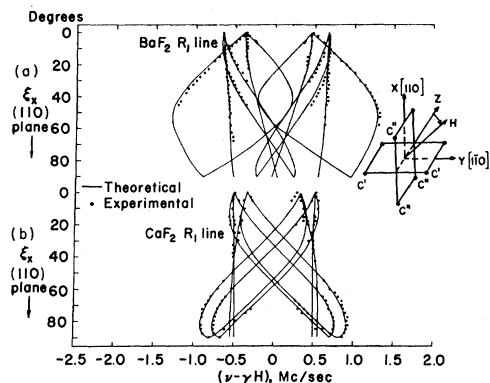


FIG. 13. (a) Angular dependence of R_1 ENDOR lines of the C nuclei in BaF_2 for the (110) rotation. (b) Angular dependence of R_1 ENDOR lines of the C nuclei in CaF_2 for the (110) rotation.

nuclei and gave rise to sufficiently well separated, distinct ENDOR lines with correct equivalences and symmetry properties. This unexpected success in explaining the BaF_2 C spectrum gave confidence for interpreting the CaF_2 lines despite the small fragments of angular dependences observed and despite mixing with the D lines. It did not appear possible to fit the D nuclei to a spin Hamiltonian, because of fragmentary data, and because, as in the case of the B nuclei, the principal axes are not determined by symmetry. Nevertheless, the D lines were clearly present and they contributed considerably to the difficulties in identifying the C lines, especially in CaF_2 . The C spectra for BaF_2 and CaF_2 are given in Fig. 13.

One further interesting development in the CaF_2 data occurred for the field parallel to the V_K center axis in the (110) rotation. As one set of C nuclei came together at about ± 0.52 Mc/sec, the line corresponding to this was observed to split just at 0° , developing a smaller satellite at about ± 0.57 Mc/sec. This violates all symmetry predictions for the C 's, so the satellite was attributed to a line from another set of nuclei. This line must split from the central packet sharply as the field approaches the V_K axis, a behavior identical to that of the A lines; this satellite was thus attributed to the E nuclei, which are located one lattice spacing beyond the A nuclei along the V_K axis (Fig. 2).